# A Molecular Orbital Calculation of Chemically Interacting Systems. Interaction between Two Radicals

Tsutomu MINATO, Shinichi YAMABE,* Hiroshi FUJIMOTO, and Kenichi FUKUI
*Faculty of Engineering, Kyoto University, Sakyo-ku, Kyoto 606*
**Department of Chemistry, Nara University of Education, Takabatake-cho, Nara 630*
(Received April 29, 1977)

The reaction path of radical-radical recombination and disproportionation has been studied by means of a perturbational method with a clear orbital interaction concept, and the mechanism of these reactions has been elucidated theoretically. It has been confirmed that these termination reactions do not have a common transition state. The recombination is found to take the path which gives the maximum interaction between the singly occupied molecular orbitals (SOMO's) of two radical species, whereas the disproportionation is shown to take the route which gives the significant charge transfer interaction from the particular doubly occupied (DO) MO of one radical to the SOMO of the other radical. The DOMO localized at the C–H bond donates electrons to the SOMO to cause the hydrogen abstraction. In the process of disproportionation, one radical which abstracts a hydrogen atom acts as an electron-acceptor and the other radical with the hydrogen atom to be abstracted as an electron-donor. The difference between the mechanism of the recombination and that of the disproportionation is clarified in terms of the mode of the orbital interaction.

When organic free radicals are generated in a reaction, the unpaired-electron species eventually undergo a termination reaction, yielding stable molecules with closed-shell electronic structures through two reaction pathways. One of them is the recombination in Eq. 1 and the other is the disproportionation with the abstraction of a hydrogen atom $\beta$ to the radical center in Eq. 2.[1]

$$\left.\begin{array}{l} RCH_2CH_2\cdot \\ + \\ R'CH_2CH_2\cdot \end{array}\right\} \begin{array}{l} \xrightarrow{k_c} RCH_2CH_2CH_2CH_2R' \quad (1) \\ \xrightarrow{k_d} RCH_2CH_3 + R'CH{=}CH_2 \quad (2) \end{array}$$

The knowledge of termination modes together with their relative rates is very important in predicting and interpreting the radical chain reactions and their products. For example, a change from recombination to disproportionation can effect a twofold variation in polymer length.

Early pictures of radical-radical reactions assumed a common transition state for the two processes of Eqs. 1 and 2, involving the excited dimer which could either be rearranged to give the disproportionation products or be quenched to give the recombination product.[2] This, however, is ruled out experimentally by a number of observations.[3] Bradley and Rabinovitch suggested an alternative interpretation of the mechanisms of the recombination and disproportionation of alkyl radicals.[4] They rejected the description of the activated complex for the disproportionation as an excited dimer and suggested that different configurations of the composite system may take part involving couplings of the radical species through three-centered hydrogen atom bonds already suggested for the recombination.[5] Consequently, the terms, "head-to-head" and "head-to-tail", used to describe the configuration of the activated complexes are discarded in the Bradley-Rabinovitch model.

$$2CH_3CH_2\cdot \longrightarrow \begin{array}{l} CH_2\cdots H \\ \| \quad \vdots \\ CH_2\cdots CH_2CH_3 \end{array} \begin{array}{l} \longrightarrow CH_3CH_2CH_2CH_3 \\ \longrightarrow CH_3CH_3 + CH_2{=}CH_2 \end{array}$$

Scheme 1.

Benson put forward the argument that both reactions, though quite different from each other, involve loose transition states with a significant ionic character.[3a]

$$2CH_3\cdot \longrightarrow \begin{array}{l} \overset{-}{C}H_3 : \overset{+}{C}H_3 \quad \text{or} \quad \overset{+1/2}{C}H_2\text{–}H\cdots\overset{-1/2}{C}H_3 \\ \longrightarrow CH_3CH_3 \end{array}$$

Scheme 2a.

$$2CH_3CH_2\cdot \longrightarrow \begin{array}{l} CH_3\overset{-}{C}H_2 : H\text{–}CH_2\overset{+}{C}H_2 \\ \text{or} \quad CH_3\overset{+}{C}H_2 : \overset{-}{H}\text{–}CH_2CH_2 \\ \longrightarrow CH_3CH_3 + CH_2{=}CH_2 \end{array}$$

Scheme 2b.

Although it is accepted that the transition states of two radical-radical termination reactions differ, there are two incompatible ways of speculation for these processes as shown in Schemes 1, 2a, and 2b. Since the reaction paths of the recombination and disproportionation are still undetermined, it seems useful to study radical destruction processes theoretically.

Recently, the $\Delta W$ method which deals with the radical-radical reacting system in terms of the molecular interaction was developed by the present authors and was applied to the recombination of two methyl radicals.[6] As the result of calculation, the interaction between both the singly occupied molecular orbitals (SOMO's) and the deformation of the methyl radical were found to be of importance for progress of the reaction. The result also demonstrates the applicability of the $\Delta W$ method further to larger reacting systems. In the present work, we have made a comparative study on the recombination and disproportionation by the use of the $\Delta W$ method. The purpose of this work is to shed light on the disputing point of the mechanism of two reaction pathways. Furthermore, the general aspect of radical-radical reaction is explained conveniently in terms of the shape of MO's of several isolated radical species, since the value of the interaction energy, $\Delta W$, is completely dependent on the overlap of MO's and gap of orbital-energy levels.

## Method of Calculation

A system composed of an ethyl radical (ER) and a methyl radical (MR) is selected as a reaction model in the $\Delta W$ method. In this reaction system the recombination gives propane and the disproportionation produces methane and ethylene.

In the $\Delta W$ method, the wave function ($\Psi$) of a chemically-interacting system between ER and MR is represented in the configuration interaction (CI) procedure:

$$\Psi = C_0\Psi_0 + \sum_{i=1}^{6}\sum_{l=5}^{7} C_{i\to l}\Psi_{i\to l} + \sum_{k=1}^{3}\sum_{j=8}^{13} C_{k\to j}\Psi_{k\to j} + \sum_{i=1}^{6} C_{i\to o'}\Psi_{i\to o'} + \sum_{k=1}^{3} C_{k\to o}\Psi_{k\to o} + \sum_{l=5}^{7} C_{o\to l}\Psi_{o\to l} + \sum_{j=8}^{13} C_{o'\to j}\Psi_{o'\to j} + C_{o\to o'}\Psi_{o\to o'} + C_{o'\to o}\Psi_{o'\to o}. \quad (3)$$

In order to describe MO's of ER and MR in their isolated states, a semiempirical all-valence-electron SCF-UHF method including overlap integrals is employed.[7] The way of estimating semiempirical parameters to evaluated MO integrals is the same as that used in a previous paper.[8] Without the lowest occupied ls-like MO, ER has six doubly occupied (DO) MO's and MR has three DOMO's. In Eq. 3, $\Psi_0$ denotes the adiabatically-interacting configuration in which neither electron transfer nor electron excitation takes place as is shown in Fig. 1. The letters "$i$" and "$j$" indicate a DOMO and an unoccupied MO, respectively, of ER, and "$k$" and "$l$" a DOMO and an unoccuppied MO, respectively, of MR. "$o$" is the SOMO of the former radical, and "$o'$" that of the latter. $\Psi_{i\to l}$ denotes a configuration of one-electron shift from the $i$-th DOMO to the $l$-th unoccuppied MO. $C_0$, $C_{i\to l}$, $C_{k\to j}$, $\cdots$, are the CI coefficients obtained by solving the usual CI secular equation. Our attention is focused on the reacting system with the singlet spin state, because in the system with the triplet spin state a radical-radical reaction is far from occurring. In this calculation, no configurations with intramolecular excitations are taken into account in Eq. 3, since it requires much more CPU time to compute the molecular integrals appearing in the CI matrix elements of the above configurations. Also, two reactants are neutral and consequently the excited configurations do not contribute as much as the charge-transferred ones to the stabilization of the reacting systems.[6]

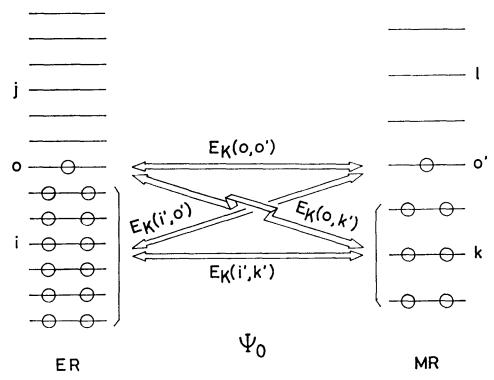


Fig. 1. The adiabatically-interacting configuration ($\Psi_0$) and the schematic representation of four types of exchange interaction between ethyl (ER) and methyl (MR) radicals. The lowest DOMO of two radicals, *i.e.*, the 1s-type one is omitted in this figure.

When the CI secular equation is expanded perturbationally, the total stabilization energy ($\Delta W$) due to the CI mentioned above can be partitioned into the following three terms, Coulomb ($E_Q$), exchange ($E_K$), and delocalization ($D$).

$$\Delta W = E_Q + E_K - D. \quad (4)$$

$E_Q$ is the classical electronic interaction energy between ER and MR. In both the singlet spin state and the triplet spin state, $E_K$ is found to be the repulsive term ($>0$) in the system of two radicals of the usual organic-chemical size. $E_K$ can be partitioned approximately into four terms.[6]

$$E_K = E_K(i',k') + E_K(i',o') + E_K(o,k') + E_K(o,o'). \quad (5)$$

In Fig. 1, four components of $E_K$ are shown schematically. $D$ is the stabilization energy due to the mixing-in of the charge transferred configurations with the adiabatically-interacting configuration. $D$ can be represented by the sum of eight components.[6]

$$D = D(i\to l) + D(k\to j) + D(i\to o') + D(k\to o) + D(o\to l) + D(o'\to j) + D(o\to o') + D(o'\to o). \quad (6)$$

In order to visualize the change of electron density along the reaction progress, a contour map of the difference electron density is given. The difference density, $\Delta\rho(1|1)_{E_K}$, of the exchange interaction is partitioned into four terms, each of which corresponds to that of the energy decomposition in Eq. 5.

$$\Delta\rho(1|1)_{E_K} = \Delta\rho(1|1)_{E_K(i',k')} + \Delta\rho(1|1)_{E_K(i',o')} + \Delta\rho(1|1)_{E_K(o,k')} + \Delta\rho(1|1)_{E_K(o,o')}. \quad (7)$$

$\Delta\rho(1|1)_{E_K(i',k')}$, for instance, indicates the difference electron density caused by the exchange interaction between both DOMO's. The difference electron density including the exchange and charge transfer (CT) interactions, $\Delta\rho(1|1)$, is also given.

Figure 2 illustrates the geometry of assumed reaction models. The geometry of the isolated ER comes from Pople's *ab initio* calculation,[9] and that of the isolated MR is referred to Herzberg's book.[10] The length of all C–H bonds and the $C_1$–$C_2$ bond of two isolated systems is kept frozen throughout the calculation. Three reaction models (I, II, and III) are shown in Fig. 2. They are distinguished by the position of MR. Models I and II represent a recombination in which MR attacks the radical center ($C_2$) of ER, MR approaching ER in the *cis*-conformation in I and in the *trans*-conformation in II. Model III represents a disproportionation in which MR attacks a hydrogen atom ($H_3$) of ER. In this calculation seven geometrical parameters are introduced to indicate various reaction processes. $\beta$ is the angle between the methylene plane (H–$C_2$–H) and $C_1$–$C_2$ bond axis of ER in Models I, II, and III. $R$ denotes the distance between $C_M$ of MR and $C_2$ of ER, and $\alpha$ is the angle between $C_M\cdots C_2$ line and the C–H bond of MR in I and II. $\theta$ and $\theta'$

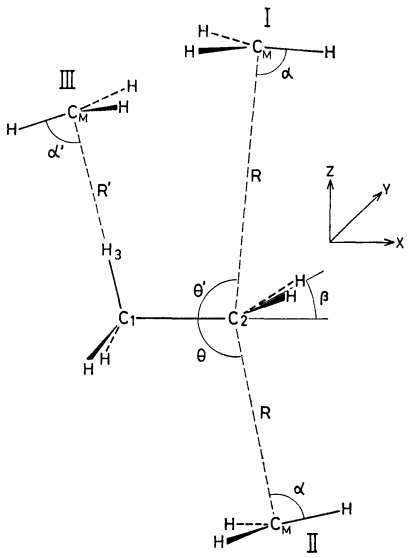


Fig. 2. Three assumed reaction models employed for the calculation of the interaction energy.

stand for the angle between $C_M \cdots C_2$ line and $C_1$–$C_2$ bond axis in Models I and II. $R'$ denotes the distance between $C_M$ of MR and $H_3$ of ER, and $\alpha'$ the angle between $C_M \cdots H_3$ line and the C–H bond of MR in Model III.

## Results of Calculation

The interaction energy ($\Delta W$) of Models I and II is given in Table 1. The $\Delta W$ of Model I ($R$=2.7 Å, $\theta'$=100°) is compared with that of Model II ($R$=2.7 Å, $\theta$=100°). We see that Model II is more favorable for the recombination. The superiority or inferiority of the recombination path is attributable to the two terms of exchange energy, $E_K(i', k')$ and $E_K(i', o')$, (see Fig. 1) and the components originating from $o$-$o'$ interaction, $E_K(o, o')$, $D(o \rightarrow o')$, and $D(o' \rightarrow o)$. Let us examine the possibility of the three-centered bond exhibited in Scheme 1. If the termination reaction proceeds along Scheme 1, the approach of MR to the $C_1$–$H_3$ bond is expected to reduce the $\Delta W$ value. In order to see the effect of this geometrical change on each energy, the angle $\theta'$ is varied tentatively from 100 to 90° in Model I. This is found to bring about a larger $\Delta W$ value, *i.e.*, destabilization of the system (Table 1). In view of the two $\Delta W$'s ($\theta'$=100, 90°) of Model I, it is realized that this destabilization comes primarily from the increase of the exchange energy, $E_K$, and slightly from the decrease of the delocalization energy, $D$. The analysis of four components of $E_K$ shows that its enlargement is due to the increase of both $E_K(i', k')$ and $E_K(i', o')$ and the decrease of the stabilizing term, $E_K(o, o')$. $D(o \rightarrow o')$ and $D(o' \rightarrow o)$ which are the stabilization energies are reduced by that variation of the geometry. The increase of $E_K(i', k')$ and $E_K(i', o')$ is due to the approach of the electronic cloud of MR to that of the $C_1$–$H_3$ bond of ER, whereas the decrease of three stabilizing terms, $E_K(o, o')$, $D(o \rightarrow o')$, and $D(o' \rightarrow o)$ is explained as follows. The SOMO of ER has a node between $C_1$ and $C_2$. As MR approaches the $C_1$–$H_3$ bond of ER, the out-of-phase overlapping of the SOMO of MR with the lobe of the SOMO of ER localized at $C_1$ and $H_3$ becomes larger. The overlap between both the SOMO's becomes small and the stabilization due to $E_K(o, o')$, $D(o \rightarrow o')$, and $D(o' \rightarrow o)$ is reduced by $\theta'$=100→90°.

Table 1. Calculated interaction energies for the recombination and disproportionation of ethyl and methyl radicals

Geometrical parameters, $R$, $R'$, $\alpha$, $\alpha'$, $\beta$, $\theta$, and $\theta'$ are those shown in Fig. 2.

| | Model I | | Model II | | Model III | |
|---|---|---|---|---|---|---|
| $R$ or $R'$ [Å] | 2.7 | 2.7 | 2.7 | 2.4 | 2.4 | 2.0 |
| $\alpha$ or $\alpha'$ [°] | 90 | 90 | 90 | 105 | 90 | 105 |
| $\beta$ [°] | 0 | 0 | 0 | 43.2 | 0 | 0 |
| $\theta$ or $\theta'$[°] | 100 | 90 | 100 | 105 | — | — |
| $E_Q$ [eV] | 0.020 | 0.022 | 0.022 | 0.069 | −0.012 | −0.033 |
| $E_K(i', k')$ | 0.459 | 0.666 | 0.394 | 0.479 | 0.180 | 0.452 |
| $E_K(i', o')$ | 0.190 | 0.227 | 0.174 | 0.338 | 0.120 | 0.428 |
| $E_K(o, k')$ | 0.072 | 0.057 | 0.087 | 0.229 | 0.010 | 0.023 |
| $E_K(o, o')$ | −0.162 | −0.141 | −0.178 | −0.622 | −0.014 | −0.047 |
| $E_K$ [eV] | 0.559 | 0.809 | 0.477 | 0.424 | 0.296 | 0.856 |
| $D(i \rightarrow l)$ | 0.003 | 0.007 | 0.003 | 0.011 | 0.001 | 0.001 |
| $D(k \rightarrow j)$ | 0.006 | 0.011 | 0.004 | 0.011 | 0.016 | 0.030 |
| $D(i \rightarrow o')$ | 0.072 | 0.089 | 0.063 | 0.108 | 0.063 | 0.233 |
| $D(k \rightarrow o)$ | 0.033 | 0.030 | 0.036 | 0.084 | 0.001 | 0.003 |
| $D(o \rightarrow l)$ | 0.003 | 0.002 | 0.003 | 0.002 | 0.000 | 0.000 |
| $D(o' \rightarrow j)$ | 0.003 | 0.003 | 0.003 | 0.002 | 0.008 | 0.019 |
| $D(o \rightarrow o')$ | 0.103 | 0.087 | 0.114 | 0.377 | 0.016 | 0.049 |
| $D(o' \rightarrow o)$ | 0.110 | 0.100 | 0.117 | 0.372 | 0.004 | 0.012 |
| $D$ [eV] | 0.333 | 0.329 | 0.343 | 0.967 | 0.109 | 0.347 |
| $\Delta W$ [eV] | 0.246 | 0.502 | 0.156 | −0.474 | 0.175 | 0.476 |

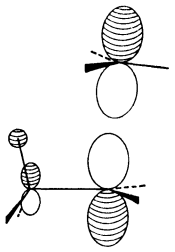
the SOMO of ER

The results show that the process of the radical destruction is not described by Scheme 1 and the recombination takes the route in which MR approaches the radical center, $C_2$, of ER in the *trans*-conformation to the $C_1$–$H_3$ bond of a methyl group of ER.

In Model II ($R$=2.4 Å, $\theta$=105°), the structural deformation of two radicals is taken into account, *i.e.*, $\alpha$=90→105° and $\beta$=0→43.2°. This deformation operates to reduce the $E_K$ and to increase the absolute value of the stabilization terms, $E_K(o, o')$, $D(o\rightarrow o')$, and $D(o'\rightarrow o)$, making the $\Delta W$ negative (Table 1). Thus, the need of the structural deformation of the radical species to promote the reaction is explicable in this MO scheme. The deformation associates the change of the extent of the hybridization ($sp^2\rightarrow sp^3$) of two radical centers, resulting in the growth of the $o$-$o'$ MO interaction which contributes overwhelmingly to the stabilization of the system. As for Model II ($R$=2.4 Å), the CI coefficients of Eq. 3 are obtained.

$$\Psi = 0.918\Psi_0 - 0.123\Psi_{o\rightarrow o'} - 0.116\Psi_{o'\rightarrow o} + \cdots. \quad (8)$$

This equation is an alternative expression of the importance of $D(o\rightarrow o')$ and $D(o'\rightarrow o)$ to promote the reaction. From the equation the transition state of the recombination hardly seems to have ionic character due to the almost equal weight of two competing ($o\rightarrow o'$ and $o'\rightarrow o$) CT interactions.

The difference density in the reaction process was investigated with respect to Model II ($R$=2.4 Å, $\theta$=105°). The density map helps us to visualize the movement of electronic cloud through some types of interactions between ER and MR. Figure 3-a shows the electron redistribution by $\Delta\rho(1|1)_{E_K(i',k')}$ caused by mutual overlap between both the DOMO's. The electron redistribution gives negative contour lines amid the $C_2\cdots C_M$ region, corresponding to the repulsive $E_K(i',k')$. The electron density maps of $\Delta\rho(1|1)_{E_K(i',o')}$ and $\Delta\rho(1|1)_{E_K(o,k')}$ are shown in Figs. 3-b and 3-c. Two terms of the exchange interaction, ($i'$, $o'$) and ($o$, $k'$), are seen to reduce the electron density along the $C_2\cdots C_M$ line, reflecting the repulsive character of $E_K(i', o')$ and $E_K(o, k')$. The last component of $\Delta\rho(1|1)_{E_K}$, $\Delta\rho(1|1)_{E_K(o,o')}$, is shown in Fig. 3-d. Since the $E_K(o, o')$ is a considerable stabilization energy (Table 1), $\Delta\rho(1|1)_{E_K(o,o')}$ is expected to give the large bonding density in the middle region between ER and MR. The expectation is confirmed by the central huge build-up of the electron density in this figure. The change of the electron distribution, $\Delta\rho(1|1)$, due to the exchange and CT interactions is shown in Fig. 3-e. It is seen that the addition of CT interaction to the exchange interaction accumulates the electron density significantly in the $C_2\cdots C_M$ region. The electron transfer from ER to MR and the compensating one from MR to ER take place equivalently, the transition state having no ionic character. This result is in line with that pointed out in Eq. 8. The trend of these electron redistributions is similar to that of the recombination of two methyl radicals.[6] From Eq. 8 and Fig. 3, the overlap of two SOMO's, the common origin of $E_K(o, o')$, $D(o\rightarrow o')$, and $D(o'\rightarrow o)$, is shown to contribute remarkably to the new bond formation.

Calculation of the $\Delta W$ was carried out with respect to Model III. The results are also given in Table 1. It should be noted that the stabilization components, $E_K(o, o')$, $D(o\rightarrow o')$, and $D(o'\rightarrow o)$, are much smaller (absolute value) in this model than in the two recombination models I and II. The difference is attributable to the fact that the SOMO of ER is localized to a greater extent at the $C_2$ atom, and the overlap between both two SOMO's in Model III is small. Of the many components of $\Delta W$ in Model III, it is $D(i\rightarrow o')$ that gives the greatest stabilization energy to the disproportionation path. Comparing the two geometries of $R'$=2.4 Å and $R'$=2.0 Å of Model III, we find that $D$ of $R'$=2.0 Å is larger than that of $R'$=2.4 Å, which is mainly due to the increase of its one component, $D(i'\rightarrow o)$, along the decrease of $R'$. The result shows that the $i\rightarrow o'$ type CT interaction becomes more important with the progress of reaction. In spite of the increase of $D$, $\Delta W$ of $R'$=2.0 Å is larger that that of $R'$=2.4 Å (Table 1). The global destabilization of Model III ($R'$=2.0 Å) is attributable to the increase of the repulsive term, $E_K$. In this calculation, the extension of the $C_1$–$H_3$ bond of ER in the course of disproportionation is not taken into account. In the realistic reaction model with the elongated $C_1$–$H_3$ bond, however, $E_K$ would become small because of the separation of MR from ethylene fragment of ER and accordingly its $\Delta W$ would be much smaller than the $\Delta W$ of Model III which has the constant $C_1$–$H_3$ bond length regardless of $R'$.

In order to find the charge-transferred configuration which contributes most to the stabilization of the reacting system, the CI coefficients are obtained with respect to Model III ($R'$=2.0 Å).

$$\Psi = 0.955\Psi_0 - 0.120\Psi_{i_4\rightarrow o'} + 0.054\Psi_{o\rightarrow o'} + 0.035\Psi_{i_5\rightarrow o'} + 0.034\Psi_{i_2\rightarrow o'} + 0.024\Psi_{o'\rightarrow o} + \cdots. \quad (9)$$

Terms, $i_2$, $i_4$, and $i_5$, denote the DOMO's of ER and suffix attached to "$i$" stands for the numbering order counted from the lowest DOMO (see Fig. 1). Equation 9 shows that the CT interaction from $i_4$ (a') to $o'$ ($a_1$) is the most important.[11] a' denotes the MO of ER within the X-Z plane belonging to the $C_s$ point group and $a_1$ the MO of MR along the $C_M\cdots H_3$ line belonging to the $C_{3v}$ point group. The $i_4$ is localized substantially at the $C_1$–$H_3$ bond and is the highest occupied (HO) MO of the C–H bond cleaved by disproportionation.

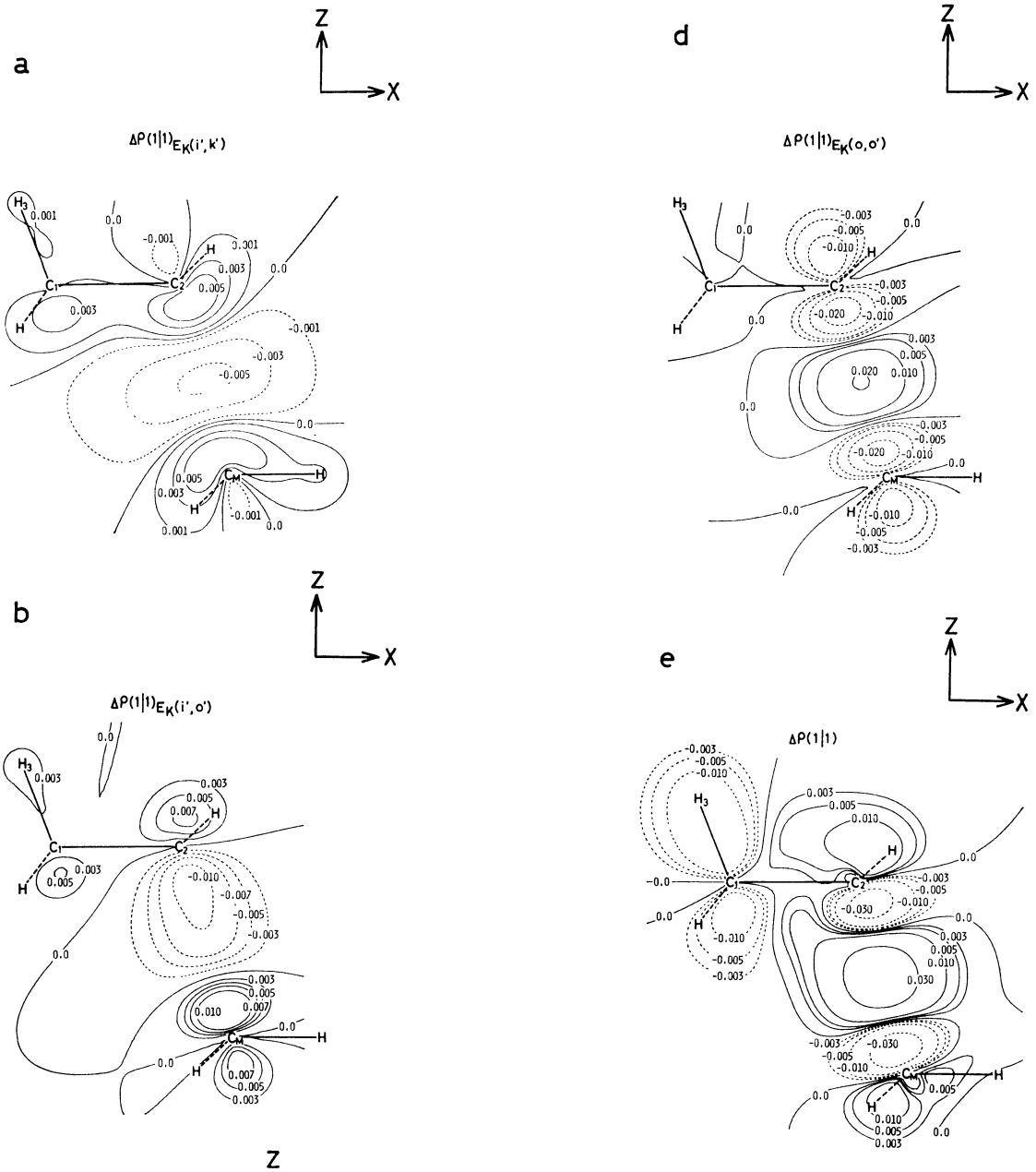


Fig. 3. The difference electron density maps of the recombination between ER and MR in Model II. The number attached to each contour line is in e/Å$^3$.

a The difference density map of $\Delta\rho(1|1)_{E_K(i',k')}$.
b The difference density map of $\Delta\rho(1|1)_{E_K(i',o')}$.
c The difference density map of $\Delta\rho(1|1)_{E_K(o,k')}$.
d The difference density map of $\Delta\rho(1|1)_{E_K(o,o')}$.
e The difference density map of $\Delta\rho(1|1)$.

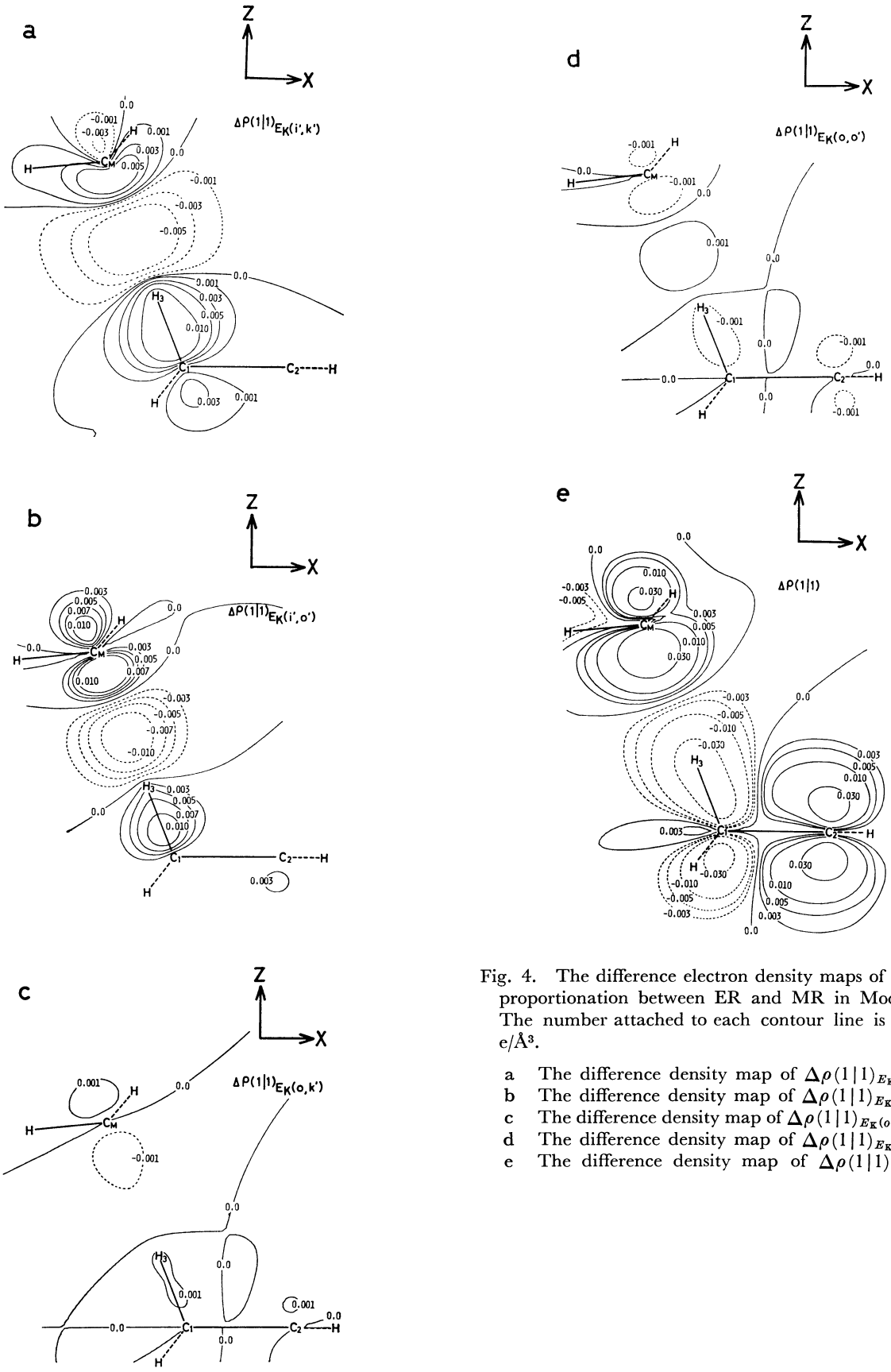


Fig. 4. The difference electron density maps of the disproportionation between ER and MR in Model III. The number attached to each contour line is also in e/Å$^3$.

a The difference density map of $\Delta\rho(1|1)_{E_K(i',k')}$.
b The difference density map of $\Delta\rho(1|1)_{E_K(i',o')}$.
c The difference density map of $\Delta\rho(1|1)_{E_K(o,k')}$.
d The difference density map of $\Delta\rho(1|1)_{E_K(o,o')}$.
e The difference density map of $\Delta\rho(1|1)$.

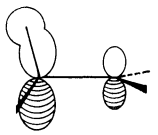

the $i_4$ MO of ER

The MO of this type is hereafter called the "C–H HOMO." In Model III representing disproportionation, this particular CT interaction plays an important role to weaken the $C_1$–$H_3$ bond through the loss of electron density of the $i_4$, forming a new $C_M \cdots H_3$ bond. From Eq. 9, MR is found to be an electron acceptor and ER to be an electron donor during the course of reaction. This donor-acceptor relation was also observed in a previous work dealing with the hydrogen abstraction reaction of a methane by a methyl radical.[12]

The electron redistribution in disproportionation is evaluated in the same way as in the recombination. Four components of $\Delta\rho(1|1)_{E_K}$ in Eq. 7 are shown separately in Fig. 4. They exhibit the same trend of electron movement as is observed in Fig. 3 of the recombination. $\Delta\rho(1|1)_{E_K(i',k')}$ (Fig. 4-a) show the large amount of the decreased density in the $C_M \cdots H_3$ region. The electron density, running away from this region, is piled up around $C_M$ and the $C_1$–$H_3$ bond. The electron density around $C_M$ resembles that of the recombination (Fig. 3-a). The density redistribution, $\Delta\rho(1|1)_{E_K(i',o')}$ (Fig. 4-b) is found to give the decreased density in the $C_M \cdots H_3$ line. Since the overlap between the SOMO of ER and any DOMO of MR is small, the change of the electron arrangement brought about by $\Delta\rho(1|1)_{E_K(o,k')}$ is expected to be minor (Fig. 4-c). The three difference densities, $\Delta\rho(1|1)_{E_K(i',k')}$, $\Delta\rho(1|1)_{E_K(i',o')}$, and $\rho\Delta(1|1)_{E_K(o,k')}$, corresponding to three repulsive energy terms of $E_K$ in Eq. 4 do not contribute to the formation of a new $C_M$–$H_3$ bond. The contour map of the electron density of $\Delta\rho(1|1)_{E_K(o,o')}$ is shown in Fig. 4-d. Since the overlap between both SOMO's is smaller in Model III than that in Model II, the density redistribution through $\Delta\rho(1|1)_{E_K(o,o')}$ is not so noticeable in the former model. Figure 4-e shows $\Delta\rho(1|1)$, representing the electron redistribution due to the exchange and CT interactions. The considerable accumulation of the electron density around $C_M$ of MR and $C_2$ of ER is observed. The diminution of the electron density appears at the $C_1$–$H_3$ bond of ER. The electron redistribution shows that the exchange and CT interactions, especially the $i_4 \rightarrow o'$ CT interaction, make electrons of ER flow into MR and that the $C_1$–$H_3$ bond is weakened by the loss of bonding electrons. The accumulated electron density around $C_M$ operates to pull the $H_3$ atom, resulting in the formation of the new $C_M$–$H_3$ bond.

The change of atomic charges in Model III ($R'$= 2.0 Å) is shown in Table 2. We see that the exchange and CT interactions make the charge on the $C_M$ atom of MR more negative and that on the $H_3$ atom of ER more positive. This indicates that the $C_M$ atom of MR has a negative charge and the $H_3$ atom of ER has a positive charge at the transition state of disproportionation. The tendency is almost similar to that suggested in the case of the disproportionation of alkoxy radicals. The result showing that the transition state of disproportionation has the ionic character is in agreement with Benson's scheme (Scheme 2b), while that of the recombination has no ionic character as shown with respect to Model II.

Table 2. Change of net charges by the exchange and CT interactions in Model III

A more negative value indicates a larger electron population.

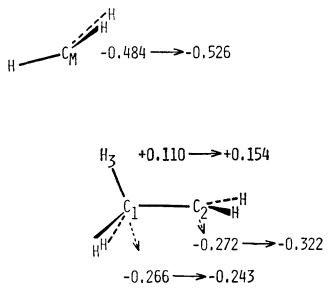


No formation of the $\pi$ bond between $C_1$ and $C_2$ of ER is observed in Fig. 4-e. The absence of the bonding component which is the origin of the $\pi$ bond in ethylene is attributable to the neglect of the excited configurations in the wave function $\Psi$ of Eq. 3. The process of the $\pi$ bond formation can be predicted qualitatively, even if the polarization effect is not taken into account explicitly. The orbitals which contribute to the $\pi$ bond formation are considered to be the $i_4$ and $o$, since all residual MO's of ER have no large $p_z$ atomic orbital (AO) component, that is, a $\pi$ bond character. A schematic representation of the $\pi$ bond formation by the orbital mixing of $i_4$ with $o$ through $o'$ is illustrated in Fig. 5.[13] The interaction of $o'$ with $o$ and $i_4$ gives the $\psi_1$, $\psi_2$, and $\psi_3$ MO's. In a DOMO, $\psi_2$, $o$, and $o'$ overlap in phase, whereas $i_4$ and $o'$ overlap

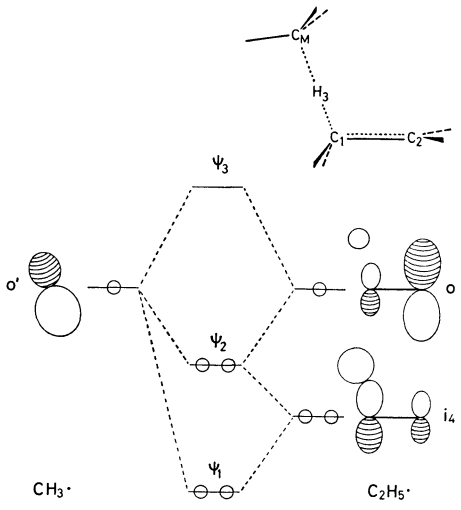


Fig. 5. The schematic representation of the $\pi$ bond formation of ethyl radical by the orbital mixing of the $i_4$ and $o$ through the $o'$. The signs of two MO's ($i_4$ and $o$) are chosen so that both of them may have positive overlap integrals with the $o'$. $\psi_2 = o - i_4 + o'$.

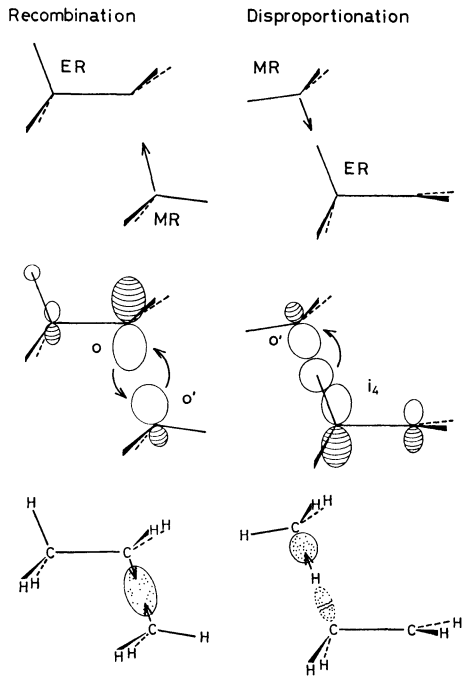


Fig. 6. Schematic representation of the reaction paths of recombination and disproportionation.

out of phase. Consequently in the $\psi_2$ orbital the interaction between the lobe at the $C_1$ atom of $i_4$ and the lobe at the $C_2$ atom of $o$ contributes to the $\pi$ bond formation. Thus, the $\pi$ bond formation of ER is explained by the orbital mixing of $i_4$ with $o$ through $o'$.

Let us summarize our results obtained so far. The reaction pathway of recombination differs a great deal from that of disproportionation, the reactions having no common transition state. This is illustrated schematically in Fig. 6. The SOMO-SOMO interaction is of importance for the progress of the reaction in recombination, whereas the CT interaction from the C–H HOMO ($i_4$) to the SOMO of one radical directed toward the hydrogen atom of the other is of importance in disproportionation. In the disproportionation, one of radical species which abstracts a hydrogen atom is an electron acceptor and the other radical species which has a hydrogen atom to be abstracted is an electron donor. Consequently the transition state of the disproportionation is expected to have an ionic character. In the recombination, however, this tendency is not observed.

## Comparison with Experimental Data

Since the interaction energy, $\Delta W$, is entirely controlled by the extent of the overlap of MO's obtained independently in two radical species, its value can be estimated roughly by analyzing the shape of these MO's. Instead of actual calculation of $\Delta W$, the reactivity of several radical species is conveniently discussed in terms of the shape of some particular MO's. In this section, the theoretical prediction given by such a simple analysis is compared with available experimental data as regards recombination and disproportionation.

*Recombination.* The simplest way in which odd-electron species are transformed into stable compounds is through the chemical bonding between the radical centers of two such species. However, in a few cases, the recombination takes an unusual path. The dimerization of cyanomethyl radical leads to a ketenimine as well as to the "normal" head-to-head dimer.[14] The former product is an unstable intermediate which rearranges quantitatively to the latter.

$$2R_2\dot{C}\text{—}CN \longrightarrow R_2C\text{—}N\text{=}C\text{=}CR_2 + R_2C(CN)\text{—}CR_2(CN)$$

In order to study the reactivity of this radical, the SOMO of cyanomethyl radical is obtained by the extended Hückel (EH) MO method.[15] The shape of the SOMO is as follows.

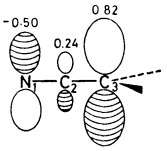


The numbers attached to each lobe denote the coefficients of the AO's of the SOMO. Judging from the shape of the SOMO of cyanomethyl radical, two recombination paths are possible. The first is the formation of the $C_3$–$C_3$ bond, giving the latter stable product, the $C_3$ atom having the largest lobe of the SOMO. The second is the linkage of the $N_1$ of one radical with the $C_3$ of the other, giving an abnormal product (ketenimine). The second mode of recombination is probably due to the following. Since $N_1$ is charged more negatively than $C_3$, reflecting the difference of electronegativity, the Coulomb long-range force represented by $E_Q$ of Eq. 4 becomes largely attractive by the approach of the $C_3\cdots N_1$. Thus, the second path of recombination is more favorable than the first in the initial stage of reaction. The abnormal recombination product is formed when the carbon radical center of one radical attacks the nitrogen atom of the other.

*Disproportionation. Isotopic Effect*: The isotopic effect is expected in the disproportionation path shown in Fig. 6. The substitution from H to D on the carbon atom adjacent to the radical center reduces the disproportionation rate constant, $k_d$, whereas in the recombination path $k_c$ does not seem to be affected so much by this substitution. In Eq. 11, isotopic substitution on the carbon atom adjacent to the radical center has a large effect on the disproportionation, but a small effect on the recombination in Eq. 10 and the disproportionation in Eq. 12. Consequently, the isotopic substitution is expected to reduce $k_d/k_c$. It is experimentally evident that in the gas, liquid, and solid phases there is a significant kinetic isotopic effect by which the substitution from H to D reduces $k_d/k_c$.[1a] Gibian and Corley measured the $k_d/k_c$ value of $C_6H_5\dot{C}HCH_3$ and $C_6H_5\dot{C}HCD_3$ in the benzene solution, and found the $[k_d/k_c(H)]/[k_d/k_c(D)]$ value to be 1.87.[16] Boddy and Steacie[17] found the $k_d/k_c$ value of $C_2D_5\cdot$ to be 0.0985 in the gase phase, and that of $C_2H_5\cdot$ 0.13,

leading to the ratio $[k_d/k_c(H)]/[k_d/k_c(D)]=1.32$. The data support the reaction paths of recombination and disproportionation assumed throughout the present work.

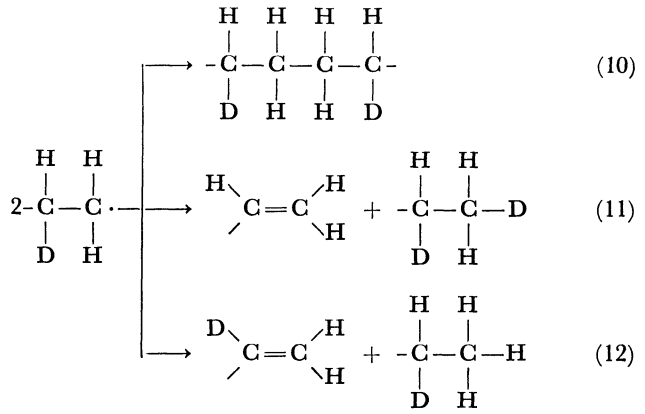

(10)

(11)

(12)

*Substitution Effect*: The CT interaction from the C–H HOMO of one radical to the SOMO of the other radical is found to be of importance to cause disproportionation. In our calculation of $\Delta W$, the former radical is ER and the latter MR. The result together with $\Delta\rho(1|1)$ of Fig. 4-e leads to the prediction that the disproportionation occurs more easily when the radical receiving an abstracted hydrogen (R) has an electron-accepting group or the radical releasing a hydrogen (R′) has an electron-donating group. Let us examine this substitution effect in more detail. For the sake of convenience, the ratio of the rate constants, $k_d/k_c$, is denoted by $\Delta$(R, R′). The number of the $\beta$-hydrogens of R′ is defined as $\beta$H. The large value of $\Delta$(R, R′)/$\beta$H indicates the ease of the occurrence of disproportionation.

Table 3 gives the $\Delta$(R, R′) of some small alkyl radical reactions.[1a] The orbital energies of the C–H HOMO of R′ are calculated by the EHMO method. The elevation of the level of the C–H HOMO corresponds to the higher reactivity of the electron-donating radical. The C–H HOMO level of the ethyl radical is found to be raised by the electron donating group. In the disproportionation between the methyl radical and the substituted ethyl radical, the $\Delta$(R, R′)/$\beta$H increases as the level of the C–H HOMO of the latter radical rises. This tendency is also observed when the ethyl radical reacts with the substituted ethyl radical (Table 3). This is also understandable from the C–H HOMO level. The inclusion of the electron acceptor group, Cl, to the R′ makes the $\Delta(CCl_3, C_2H_4Cl)/\beta H$ smaller than the $\Delta(CCl_3, C_2H_5)/\beta H$. Although the recombination is assumed to be uninfluenced by the substitution effect, the trend of the above data suggests that the disproportionation rate constant is affected by the energy gap between the SOMO of the radical receiving the hydrogen atom and the C–H HOMO of the radical releasing the hydrogen atom when the height of the SOMO is kept frozen.

Table 3. Ratio of rate constants with the substitution effect

| R | R′ | $\Delta$(R, R′) | $\Delta$(R, R′)/$\beta$H | HOMO level[a] (eV) |
|---|---|---|---|---|
| $CH_3\cdot$ | $CH_3CH_2\cdot$ | 0.039 | 0.012 | −15.18 |
| | $CH_3CH_2CH_2\cdot$ | 0.058 | 0.029 | −14.00 |
| | $(CH_3)_2CHCH_2\cdot$ | — | — | −13.38 |
| $C_2H_5\cdot$ | $CH_3CH_2\cdot$ | 0.065 | 0.022 | −15.18 |
| | $CH_3CH_2CH_2\cdot$ | 0.066 | 0.033 | −14.00 |
| | $(CH_3)_2CHCH_2\cdot$ | 0.04 | 0.04 | −13.38 |
| $CCl_3\cdot$ | $CH_3CH_2\cdot$ | 0.22 | 0.073 | −15.18 |
| | $CH_2ClCH_2\cdot$ | 0.14 | 0.070 | −15.23 |

a) The calculated orbital energy of the C–H HOMO (see Text) is indicated.

*Solvent Effect*: The density map, $\Delta\rho(1|1)$, (Fig. 4-e) shows that the transition state of the disproportionation is polarized in spite of the reaction of two neutral radicals, but not that of recombination. This leads to the expectation that the disproportionation is accelerated in polar solvents, but not recombination. Stefani measured the ratio of the rate constants, $k_d/k_c$, for the termination reaction of ethyl radicals in various sol-

Table 4. Disproportionation-recombination of ethyl radicals as a function of solvents[a]

| | Scavenger | $k_d/k_c$ | $\delta$[b] | $\Omega$ | $Z$[c] | $E_T$[c] |
|---|---|---|---|---|---|---|
| Gas phase | None | 0.14 | | | | |
| Isooctane | None | 0.144±0.003 | 48 | | 60.1 | |
| Isooctane | Styrene | 0.145±0.007 | 48 | | 60.1 | |
| Limonene | None | 0.158±0.005 | 56 | | | |
| Ethylbenzene | None | 0.156±0.001 | 59 | | | |
| *m*-Xylene | None | 0.165±0.003 | 61 | | | |
| Toluene | None | 0.167±0.003 | 62 | | | 33.9 |
| 2-Butanol | None | 0.168±0.003 | 68 | | | |
| 2-Propanol | Styrene | 0.178±0.001 | 70 | | 76.3 | 48.6 |
| 1-Propanol | Styrene | 0.181±0.003 | 72 | | 78.3 | 50.7 |
| Aniline | Styrene | 0.195±0.001 | 75 | | | 44.3 |
| Acetonitrile | None | 0.200±0.006 | 83 | 0.692 | 71.3 | 46.0 |
| Acetonitrile | Styrene | 0.208±0.006 | 83 | 0.692 | 71.3 | 46.0 |
| Ethylene glycol | None | 0.241±0.003 | 97 | | 85.1 | 56.3 |

a) From Ref. 18. b) Estimated from Fig. 1 of Ref. 18. c) *Cf.*, M. Seno and T. Arai, "Yukikagakuhanno Ni Okeru Yobaikoka," ed by T. Asahara, Sangyotosho, Tokyo (1970).

vents.[18] He found that $\log(k_d/k_c)$ is a linear function of $\sqrt{\delta}$ where $\delta$ is the Hildebrand solubility parameter, expressing the internal pressure of the solvent.[19] Herbrandson and Neufeld proposed[20] that $\delta$ correlated with various polarity parameters such as $Y$,[21] $\Omega$,[22] $Z$,[23] and $E_T$.[24] The values of $k_d/k_c$, $\delta$, and these four polarity parameters are given in Table 4. The larger the values of the parameters, the larger the solvent polarity. The transition state of disproportionation is expected to have a polar character to be stabilized by the solvent. This is in line with our proposal of the different ionic characters of recombination and disproportionation.

Alkoxy radicals are known to give very high fractions of disproportionation in comparison with alkyl radicals.[1a] It is suggested that this phenomenon is attributable to the increased polar conditions by an electronegative oxygen atom at the transition state.[25]

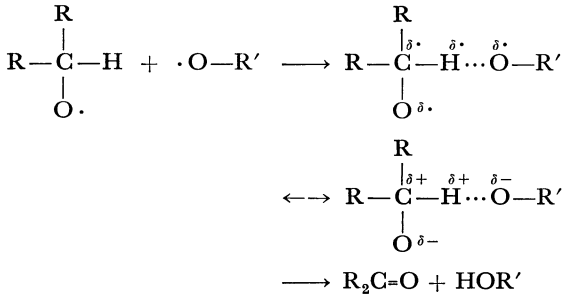

The suggestion that the transition state of the disproportionation of alkoxy radicals has an ionic character supports our view of the transition state of the disproportionation of alkyl radicals.

## Conclusion

Recombination, one of two termination reactions, takes a reaction path differing from that of the other termination reaction, disproportionation. These two reactions are shown to have no common transition state. The recombination path is the route by which two radicals approach in such a direction that the overlap between both SOMO's may become maximum. It is suggested that the transition state of recombination is not much polarized. The disproportionation path is the route by which one radical receiving a hydrogen atom attacks the $\beta$ hydrogen atom of the other radical. The CT interaction from the C–H HOMO of one radical to the SOMO of the other abstracting a hydrogen atom plays an important role to cause disproportionation. The radical receiving a hydrogen atom is found to be an electron acceptor and the radical with the C–H bond broken in the disproportionation an electron donor. The transition state of disproportionation is shown to have a polar character.

We would like to express our gratitude to the staff of the Data Processing Center, Kyoto University, for permission to use the FACOM 230-75 computer. The MO calculation was carried out with financial support of the Ministry of Education (Grant-in-Aid 139012).

## References

1) (a) M. J. Gibian and R. C. Corley, *Chem. Rev.*, **73**, 441 (1973); (b) J. A. Kerr, "Free Radicals," Vol. 1, ed by J. K. Kochi, John Wiley & Sons, New York, N. Y. (1973).
2) J. A. Kerr and A. F. Trotman-Dickenson, *Prog. React. Kinet.*, **1**, 107 (1961).
3) (a) S. W. Benson, *Adv. Photochem.*, **2**, 1 (1964); (b) H. A. Gillis, *Can. J. Chem.*, **49**, 2861 (1971).
4) J. N. Bradley and B. S. Rabinovitch, *J. Chem. Phys.*, **36**, 3498 (1962).
5) O. K. Rice, *J. Phys. Chem.*, **65**, 1588 (1961).
6) S. Yamabe, T. Minato, H. Fujimoto, and K. Fukui, unpublished result (1977).
7) T. Yonezawa, K. Yamaguchi, and H. Kato, *Bull. Chem. Soc. Jpn.*, **40**, 536 (1967).
8) K. Fukui, H. Fujimoto, and S. Yamabe, *J. Phys. Chem.*, **76**, 232 (1972).
9) W. A. Lathan, W. J. Hehre, and J. A. Pople, *J. Am. Chem. Soc.*, **93**, 808 (1971).
10) G. Herzberg, "Molecular Spectra and Structure," D. Van Nostrand Co., New York (1966).
11) It should be noted that when a radical receiving a hydrogen atom has a high-lying SOMO, or a radical giving a hydrogen atom has the lowest unoccupied (LU) MO with a very low energy localized at the C–H bond, the CT interaction from the SOMO to the LUMO could be more important than that from the particular DOMO to the SOMO.
12) H. Fujimoto, S. Yamabe, T. Minato, and K. Fukui, *J. Am. Chem. Soc.*, **94**, 9205 (1972).
13) S. Inagaki, H. Fujimoto, and K. Fukui, *J. Am. Chem. Soc.*, **98**, 4054 (1976).
14) (a) C. G. Hammond, O. D. Trapp, R. T. Keys, and D. L. Neff, *J. Am. Chem. Soc.*, **81**, 4878 (1959); (b) G. Ayrey, K. L. Evans, and D. J. D. Wong, *Eur. Polym. J.*, **9**, 1347 (1973).
15) R. Hoffmann, *J. Chem. Phys.*, **39**, 1397 (1963).
16) M. J. Gibian and R. C. Corley, *J. Am. Chem. Soc.*, **94**, 4178 (1972).
17) P. J. Boddy and E. W. Steacie, *Can. J. Chem.*, **38**, 1576 (1960).
18) A. P. Stefani, *J. Am. Chem. Soc.*, **90**, 1694 (1968).
19) J. H. Hildebrand and R. L. Scott, "Regular Solutions," Prentice-Hall, Inc., Englewood Cliffs, N. J. (1962).
20) H. F. Herbrandson and F. R. Neufeld, *J. Org. Chem.*, **31**, 1140 (1966).
21) A. H. Fainberg and S. Winstein, *J. Am. Chem. Soc.*, **78**, 2770 (1956).
22) J. A. Berson, Z. Hamlet, and W. A. Mueller, *J. Am. Chem. Soc.*, **84**, 297 (1962).
23) E. M. Kosower, *J. Am. Chem. Soc.*, **80**, 3253 (1958).
24) K. Dimroth, C. Reichardt, T. Siepmann, and F. Bohlmann, *Ann. Chem.*, **661**, 1 (1963).
25) D. F. Dever and J. G. Calvert, *J. Am. Chem. Soc.*, **84**, 1362 (1962).